Pressure-Dependent ZnO Nanocrsytal Growth in a Chemical Vapor Deposition Process

B. P. Zhang,*,†,‡ N. T. Binh,† K. Wakatsuki,†,‡ Y. Segawa,†,‡ Y. Yamada,§ N. Usami,§ M. Kawasaki,§ and H. Koinuma⊥

Photodynamics Research Center, The Institute of Physical and Chemical Research (RIKEN), 519-1399 Aoba, Aramaki, Aoba-ku, Sendai 980-0845, Japan, Department of Physics, Graduate School of Science, Tohoku University, Sendai 980-8578, Japan, Institute for Materials Research, Tohoku University, Sendai 980-8577, Japan, and Materials and Structures Laboratory, Tokyo Institute of Technology, Yokohama 226-8503, Japan

Received: March 31, 2004; In Final Form: May 13, 2004

By using metalorganic chemical vapor deposition, ZnO nanorods, nanotubes, and nanowalls can be selectively obtained by adjusting the growth pressure from 10 to 0.06 Torr. The appearance of different nanostructures is due to different growth modes. The variation of nanostructure shape with change in pressure is explained in terms of surface-to-volume ratio. Photoluminescence measurements show that growth at low-pressure facilitates the incorporation of acceptors in ZnO.

Introduction

As a light-emitting material in the ultraviolet spectral region, ZnO has been extensively studied. ZnO is characterized by a large exciton binding energy (60 meV), which is more than two times the value of thermal energy at room temperature. As a result, when crystalline quality is high, stable exciton states are achievable at room temperature and exciton-involved stimulated emission processes, which can lead to highly efficient photonic devices, have been demonstrated.[1] ZnO is also useful in many other devices such as solar cells,[2] sensors,[3] varistors,[4] surface acoustic wave devices,[5] and hydrogen-storage devices.[6] The use of nanoscaled ZnO structures is expected to improve the performance of such devices. A review on ZnO nanostructures has been given by Dai et al.[7] Various ZnO nanostructures such as quantum wells,[8] nanodots,[9] nanowires/nanorods,[10,11] nanobelts,[12] nanonails,[13] nanobridges,[13] nanowalls,[14,15] and nanotubes[16,17] have been reported. Methods that have been used to fabricate ZnO nanostructures include molecular beam epitaxy,[8] metalorganic chemical vapor deposition (MOCVD),[9,10] thermal evaporation,[11−16] and solution-phase process.[17]

In this paper, fabrication of ZnO nanorods, nanotubes, and nanowalls by using MOCVD is reported. MOCVD, a technique widely used in industry, enables growth at a low temperature, does not require a catalyst and enables epitaxial growth. Single-crystal ZnO nanorods have been fabricated on sapphire (0001) and (11$\bar{2}$0) substrates by using methods of thermal evaporation and MOCVD. Emissions due to biexcitons and lasing due to exciton−exciton scattering from ZnO nanorods have been observed.[10,11] ZnO nanorods are also good candidates for field-emission devices.[18] ZnO nanotubes and nanowalls, however, have not been extensively studied. Nanotubes reported previously were either polycrystalline[17] or amorphous[16] and had random growth directions. Single-crystal ZnO nanowalls have been fabricated by using the thermal evaporation method on sapphire (11$\bar{2}$0) substrates. The formation of nanowalls was based on a vapor−liquid−solid growth mode with a catalyst, and the growth temperature was high (875−950 °C).[14,15]

We obtained ZnO nanorods, nanotubes, and nanowalls on sapphire (0001) substrates by simply adjusting the growth pressure. It was found that nanostructures change in the order of nanorods, nanotubes, and nanowalls with a decrease in growth pressure from 10 to 0.06 Torr.

The nanostructures were all grown epitaxially and had the same epitaxial relationship with respect to the substrate. The growth technique used in the present study is characterized by a low growth temperature (350−500 °C) and does not require the use of a catalyst.

Experimental Section

The growth was carried out with the same MOCVD system as that used in our previous study.[10] It consists mainly of a horizontal stainless chamber, a turbo molecular pump (TMP), and a rotary pump. A remote-controlled conductance valve was placed between the chamber and the TMP to control chamber pressure. Oxygen gas (O_2) and diethyl zinc (DEZn, $Zn(C_2H_5)_2$) were used as precursors. The carrier gas for DEZn was nitrogen. To prevent pre-reaction between precursors, DEZn was conducted directly to the substrate surface by using a stainless nozzle. On the other hand, O_2 was conducted by two pathways, one being directly to the substrate surface with a stainless nozzle. The nozzles inside the growth chamber can be removed for cleaning after a certain amount of growth. Substrate temperature was controlled by adjusting the output power of lamp heaters installed beneath a susceptor made of inconel 600. Sapphire (0001) substrates were cleaned in an ultrasonic bath of organic solutions and then placed on the susceptor. At room temperature, O_2 flow was started and the reactor pressure, P_v, was controlled in the range of 0.06−10 Torr. Then the substrate was heated to 400−500 °C and DEZn was introduced to start the growth. The flows of O_2 and N_2 were set to 30 sccm (including 10 sccm from the nozzle pathway) and 5 sccm, respectively. The temperature of DEZn was 3−6 °C. During the whole process,

* Address correspondence to this author. E-mail: bzhang@postman.riken.go.jp.
† The Institute of Physical and Chemical Research (RIKEN).
‡ Department of Physics, Graduate School of Science, Tohoku University.
§ Institute for Materials Research, Tohoku University.
⊥ Tokyo Institute of Technology.

10.1021/jp048602i CCC: $27.50
Published on Web 06/19/2004

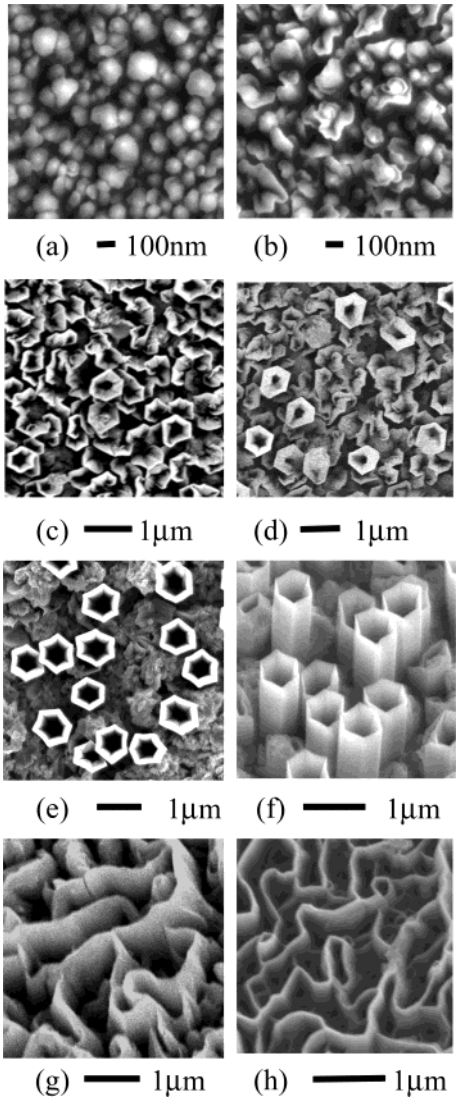

Figure 1. SEM surface images of ZnO nanostructures after 1 h of growth under different growth pressures: (a) 10, (b) 6, (c) 3, (d) 1, (e) 0.6, (f) 0.3, (g) 0.1, and (h) 0.06 Torr. The structure changes from nanorods to nanotubes and then nanowalls. Panels a to e were the top images and panels f to g were taken with an inclination angle.

P_v was kept at the same value. The surface morphology was examined with use of a scanning electron microscope (SEM). The crystalline property was characterized with a triple-axis, four-crystal X-ray diffractometer (XRD). Photoluminescence (PL) measurements were carried out to study optical properties by exciting the sample with an He−Cd 325-nm laser. The luminescence was dispersed by a monochromator and detected by a charge-coupled device (CCD). The sample temperature was 4.2 K.

Results and Discussion

Figure 1 shows SEM images of ZnO nanostructures grown under various values of P_v. With decreasing P_v, the ZnO nanostructures changed from nanorods to nanotubes and then nanowalls. In our experiments, ZnO nanorods, nanotubes, and nanowalls were obtained at $P_v = 10-6$, $1-0.3$, and $0.1-0.06$ Torr, respectively. The diameters of the nanorods formed at 10 Torr (Figure 1a) ranged from 30 to 100 nm. The formation of ZnO nanorods can be attributed to the overall effect of the three-dimensional (3D) growth mode and the difference between growth rates of ZnO in different directions.[19] At $P_v = 6$ Torr (Figure 1b), some of the rods changed to a spiral columnar growth mode. This growth mode has been demonstrated in a superconducting material, $YBa_2Cu_3O_7$.[20] When the pressure was decreased to 3 Torr (Figure 1c), the columns became tube-like structures, probably due to the preferred growth at the edge of a spirally rising step.[20] At $P_v = 1$ Torr, some of the tube-like columns emerge higher with hexagonal shapes. Further reduction of P_v to 0.6 and to 0.3 Torr resulted in an increase in the number of nanotubes, and interestingly, all the hexagonal nanotubes had the same in-plane orientations. The diameters and wall thickness of the nanotubes were about 500 and 100 nm, respectively. When P_v was reduced to $0.1-0.06$ Torr, ZnO nanowalls were obtained. The nanowalls had thicknesses of $50-100$ nm and had formed networks.

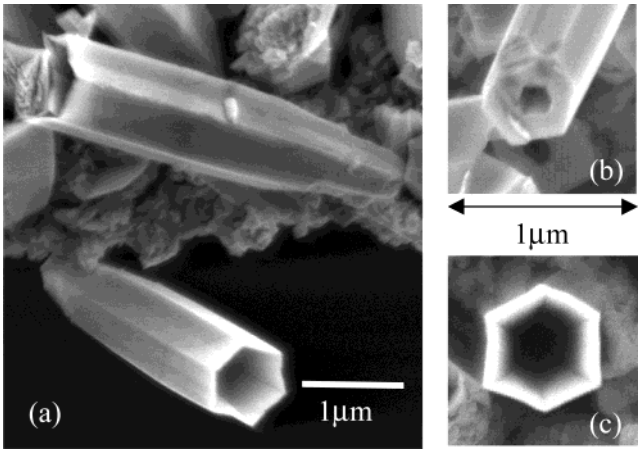

Figure 2. SEM images of two single nanotubes (a) and the bottom (b) and the top (c) of a single nanotube.

Figure 2 shows the SEM images of two single nanotubes, including the images of the cross sections of the top and bottom. The total length was up to 5 μm. It is clear that, at the initial stage of growth, the diameter of a nanotube increases largely within a length of $1-2$ μm. This can explain the size variation from nanorods to nanotubes. Except for this size-growing region, the tube size was uniform in the remaining ~ 3 μm length. The images of the cross sections shown in panels b and c of Figure 2 also demonstrate the variation of the inner diameter from ~ 200 nm at the bottom to ~ 400 nm at the top.

The pressure-driven evolution of nanostructures indicates that nanotubes originate from a spiral-columnar growth mode. However, the rapid change from nanotubes to nanowalls makes it difficult to obtain information on the growth mode for the latter. To confirm the growth mechanism of the nanowalls, samples with different film thicknesses were also prepared. Figure 3 shows the evolution of surface images of samples prepared under growth conditions of nanowalls. Nanoscale grains of $20-50$ nm were observed when the film was thin. With an increase in film thickness, some of the nanograins began to connect via bridges. With a further increase in growth time, the bridges became walls and, simultaneously, new bridges were also created. Finally, networks of nanowalls were formed. These observations show that different pressures cause different growth modes. The origin of the bridges is still not clear. Previous studies showed that ZnO nanowalls can be formed by a VLS growth mode.[14,15] Since no catalyst was used, this VLS mode should not be responsible for the formation of nanowalls in this study.

XRD measurements demonstrated that all of these nanostructures grew with the *c*-axis perpendicular to the substrate surface. This is because the top (0001) surface has the lowest level of

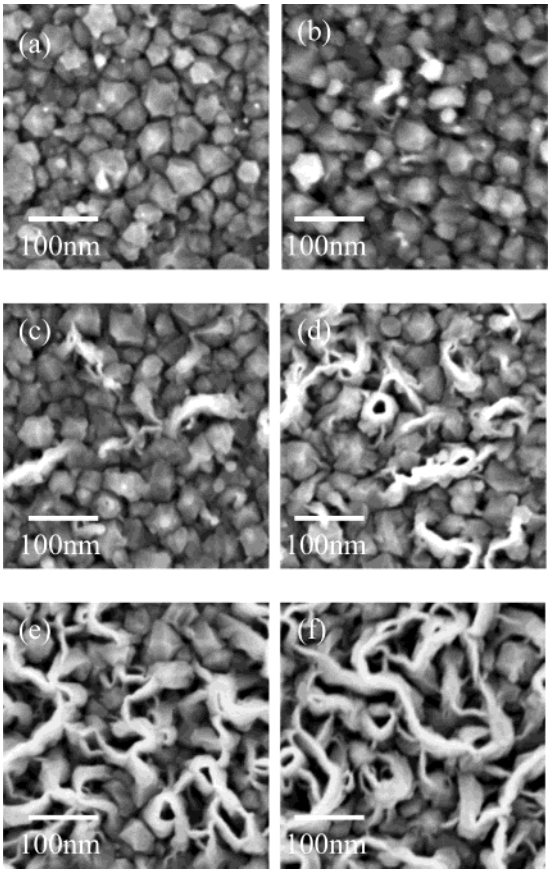

Figure 3. SEM surface images of samples grown under conditions of nanowalls with different thickness. The thickness increases in the order from panel a to panel f.

surface energy (0.099 eV/Å^2) and, in an equilibrium state, the crystal grows with this plane parallel to the substrate surface.[21] Figure 4a shows XRD rocking curves of ZnO (0002) crystal planes obtained from different kinds of nanostructures. The full-width-at-half-maximum (fwhm) values ranged from 0.47° to 2.1°, indicating that all of the nanostructures were grown with good alignment. Figure 4b shows Φ scan spectra of ZnO $\{11\bar{2}2\}$ planes of different nanostructures along with those of sapphire $\{11\bar{2}6\}$ planes. Six peaks with equal 60° intervals were obtained from all of the nanostructures, though they have different shapes, and their peaks are shifted 30° from those of the substrate. It is thus clear that ZnO nanorods, nanotubes, and nanowalls are all grown epitaxially and have the same epitaxial relationships with respect to the substrate.

PL spectra of various nanostructures obtained at 4.2 K are shown in Figure 5. The spectra are displayed in the order of decreasing P_v from 10 (top) to 0.06 Torr (bottom). The peak at 3.366 eV is common to all nanostructures (or all values of P_v) and is attributed to neutral-donor-bound excitons (D^0X). In addition, a few peaks were observed depending on the P_v value or the nanostructure. The origin of the peak at 3.333 eV, observed when $P_v = 0.6-10$ Torr, may be due to acceptor-bound excitons.[22] The peak located at 3.312−3.318 eV is due to donor−acceptor pairs (DAP) with an acceptor binding energy of 107 meV[10] or 124 meV.[23] A general trend is that the DAP-to-D^0X intensity ratio becomes larger with a decrease in P_v. This indicates that growth at lower pressure in MOCVD may enhance the incorporation of acceptors in ZnO. Spontaneous doping of nitrogen, which is known to act as an acceptor, might have taken place in these structures. The origin of the broad

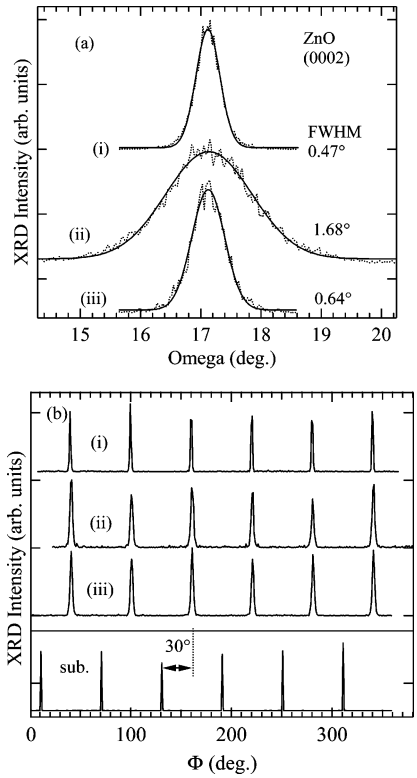

Figure 4. Typical XRD rocking curves (a) of ZnO (0002) planes and Φ scans (b) of ZnO $(11\bar{2}2)$ planes of different nanostructures. In panel a, dotted curves are measured results and solid ones are fitted results, using Gaussian profiles. In both panels a and b, the growth pressures were (i) 10, (ii) 0.3, and (iii) 0.06 Torr, corresponding to nanorods, nanotubes, and nanowalls, respectively. Each spectrum was normalized by its maximum intensity. The bottom spectrum in panel b is the Φ scan of Al_2O_3 $(11\bar{2}6)$ planes of the substrate.

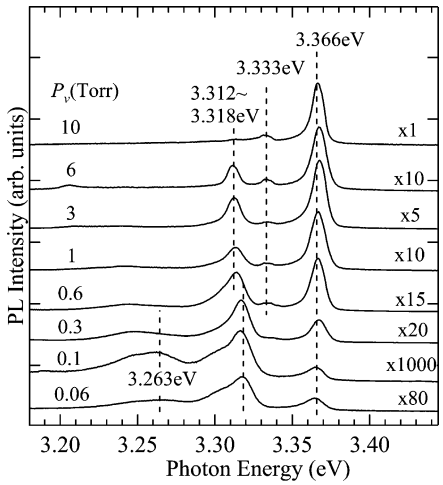

Figure 5. Low-temperature PL spectra of different nanostructures. The peaks at 3.366 and 3.312−3.318 eV are due to D^0X and DAP, respectively. With a reduction in the growth pressure, the DAP-to-D^0X intensity ratio becomes larger, which suggests an increased acceptor concentration.

band at 3.263 eV, which was observed from ZnO nanowalls, is not clear at present.

It is obvious that the chamber pressure P_v plays an important role: growth of nanorods, nanotubes, and nanowalls can be controlled by adjusting the growth pressure. A nanostructure can be regarded as a nonflat, small volume crystal. The crystal shape depends on the surface energy. If an equilibrium process is assumed at each pressure, the condition for equilibrium is

given by the minimum of the Helmholtz free energy of the system, which results in[24]

$$P_c - P_v = \sum_i \delta(\sigma_i S_i)/\delta V_c \quad (1)$$

where P_c is the inner pressure of the crystal phase, σ_i and S_i are the density of surface energy and the area of the surface i, respectively, V_c is the volume of the crystal phase, and i indicates different surfaces for a small crystal.

When the crystalline facets are the same for different nanostructures, eq 1 indicates that a lower chamber pressure facilitates a higher surface-to-volume ratio. This is exactly what we have observed. The formation of nanorods at 10 Torr can be attributed to the overall effect of both the 3D growth and the anisotropic growth rate. Due to the large lattice mismatch between ZnO and the substrate, ZnO will not obey a two-dimensional layer-by-layer growth mode that results in the formation of flat films. The 3D growth mode causes surface roughness, which finally causes formation of nanorods due to the higher growth rate along the *c*-axis.[19] When the chamber pressure was decreased to 6 Torr, spiral columnar growth took place. At 3 Torr, some of the nanorods began growing in a hollow, hexagonal shape, by which a larger surface-to-volume ratio is possible. With a further decrease in pressure to 0.3 Torr, most of the structures became nanotubes with perfect hexagonal cross sections and possessed uniform diameters and the same in-plane orientations. When the pressure was decreased further to 0.1 and to 0.06 Torr, nanowalls, by which an even higher surface-to-volume ratio is achieved, were obtained.

To examine the initial nucleation, growths under different pressures were performed with changes in the growth time. Figure 3 demonstrates that nanometer-scaled ZnO islands are formed at the initial stage under the growth condition of nanowalls. In fact, such behavior is also true for nanorods and nanotubes. In other words, the initial nucleation of ZnO is similar for different nanostructures. Our opinion is the following: The initial nucleation is dependent on both the growth condition (substrate temperature, reactor pressure, etc.) and the film−substrate lattice mismatch. In our study where the substrate temperature is fixed, the main factors affecting the growth mode will be the reactor pressure and the lattice mismatch. In the case of ZnO growing on a sapphire (0001) substrate, the lattice mismatch is very large (~18%) and the effect of lattice mismatch is dominant. Therefore, the Volmer−Weber growth mode is expected, which causes three-dimensional clusters at the initial stage of growth.[25] As growing continues, the island size increases and the lattice mismatch can be relaxed by formation of defects. After relaxation, the effect of lattice mismatch is weakened and the pressure changes to be the dominant factor determining the growth characteristics. It is believed that both the defect type and the succeeding growth of ZnO are dependent on the reactor pressure, which leads to different nanostructures. In our experiments, when the effective thickness is larger than 1 μm, we can constantly obtain nanorods, nanotubes, or nanowalls by simply selecting the reactor pressure. In any case, the surface morphology is homogeneous, i.e., there is only one type of nanostructure on the whole 10×10 mm^2 substrate.

Nanorods and nanotubes can be used in nanoscale UV lasers and field-emission devices. Nanotubes and nanowalls, for which the total surface area is much larger than the area of a flat surface, can be used in energy-storage devices, sensors, and dye-sensitized solar cells. The characteristics of single crystal and good alignment are important for realization of lasing cavity, high efficiency, and fast response of these devices.

Conclusion

ZnO nanorods, nanotubes, and nanowalls were selectively obtained by controlling the reactor pressure in growth by MOCVD. These nanostructures were all epitaxially grown and had the same epitaxial relationship with respect to the substrate. Mechanisms corresponding to different nanostructures were discussed. The variation in nanostructure shape with change in pressure was discussed in terms of surface-to-volume ratio. Growth at lower pressures was found to enhance the incorporation of acceptors in ZnO, which gives guidance toward realization of p-type ZnO.

References and Notes

(1) Zu, P.; Tang, Z. K.; Wong, G. K. L.; Kawasaki, M.; Ohtomo, A.; Koinuma, H.; Swgawa, Y. *Solid State Commun.* **1997**, 103, 459.
(2) Katoh, R.; Furube, A.; Hara, K.; Murata, S.; Sugihara, H.; Arakawa, H.; Tachiya, M. *J. Phys. Chem. B* **2002**, *106*, 12957.
(3) Roy, S.; Basu, S. *Bull. Mater. Sci.* **2002**, *25*, 513.
(4) Ohashi, N.; Kataoka, K.; Ohgaki, T.; Miyagi, T.; Haneda, H.; Morinaga, K. *Appl. Phys. Lett.* **2003**, *83*, 4857.
(5) Sharma, P.; Kumar, S.; Sreenivas, K. J. *Mater. Res.* **2003**, *18*, 545.
(6) Wan, Q.; Lin, C. L.; Yu, X. B.; Wang, T. H. *Appl. Phys. Lett.* **2004**, *84*, 124.
(7) Dai, Z. R.; Pan, Z. W.; Wang, Z. L. *Adv. Funct. Mater.* **2003**, *13*, 9.
(8) Chia, C. H.; Makino, T.; Tamura, K.; Segawa, Y.; Ohtomo, A.; Koinuma, H. *Appl. Phys. Lett.* **2003**, *82*, 1848.
(9) Kim, S. W.; Fujita, Sz.; Fujita, Sg. *Appl. Phys. Lett.* **2002**, *81*, 5036.
(10) Zhang, B. P.; Binh, N. T.; Segawa, Y.; Wakatsuki, K.; Usami, N. *Appl. Phys. Lett.* **2003**, *83*, 1635.
(11) Huang, M. H.; Mao, S.; Feick, H.; Yan, H.; Wu, Y.; Kind, H.; Weber, E.; Russo, R.; Yang, P. *Science* **2001**, *292*, 1897.
(12) Pan, Z. W.; Dai, Z. R.; Wang, Z. L. *Science* **2001**, *291*, 1947.
(13) Lao, J. Y.; Huang, J. Y.; Wang, D. Z.; Ren, Z. F. *Nano Lett.* **2003**, *3*, 235.
(14) Ng, H. T.; Li, J.; Smith, M. K.; Nguyen, P.: Cassell, A.; Han, J.; Meyyappan, M. *Science* **2003**, *300*, 1249.
(15) Lao, J. Y.; Huang, J. Y.; Wang, D. Z.; Ren, Z. F.; Steeves, D.; Kimball, B.; Porter, W. *Appl. Phys. A* **2004**, *78*, 539.
(16) Hu, J.; Bando, Y.; Liu, Z. *Adv. Mater.* **2003**, *15*, 1000.
(17) Zhang, J.; Sun, L.; Liao, C.; Yan, C. *Chem. Commun.* **2002**, 262.
(18) Xu, C. X.; Sun, X. W. *Appl. Phys. Lett.* **2003**, *83*, 3806.
(19) Muthukumar, S.; Sheng, H.; Zhong, J.; Zhang, Z.; Emanetoglu, N. W.; Lu, Y. *IEEE Trans. Nanotechnol.* **2003**, *2*, 50.
(20) Hawley, M.; Raistrick, I. D.; Beery, J. G.; Houlton, R. J. *Science* **1991**, *251*, 1587.
(21) Fujimura, N.; Nishihara, T.; Goto, S.; Xu, J.; Ito, T. *J. Cryst. Growth* **1993**, *130*, 269.
(22) Kato, H.; Sano, M.; Miyamoto, K.; Yao, T. *Jpn. J. Appl. Phys.* **2003**, *42*, 2241.
(23) Zhao, Q. X.; Willander, M.; Morjan, R. E.; Hu, Q. H.; Campbell, E. E. B. *Appl. Phys. Lett.* **2003**, *83*, 165.
(24) Markov, I. V. *Crystal Growth for Beginners, Fundamentals of Nucleation, Crystal Growth and Epitaxy*; World Scientific: Singapore, 1996, p 13.
(25) Floro, J. A.; Hearne, S. J.; Hunter, J. A.; Kotula, P.; Chason, E.; Seel, S. C.; Thompson, C. V. *J. Appl. Phys.* **2001**, *89*, 4886.